

Low-depth circuit ansatz for preparing correlated fermionic states on a quantum computer

Pierre-Luc Dallaire-Demers,¹ Jonathan Romero,² Libor Veis,³ Sukin Sim,² and Alán Aspuru-Guzik^{2,4}

¹*Xanadu, 372 Richmond St W, Toronto, M5V 2L7, Canada*

²*Department of Chemistry and Chemical Biology, Harvard University, Cambridge MA, 02138*

³*J. Heyrovský Institute of Physical Chemistry, ASCR, 18223 Prague, Czech Republic*

⁴*Senior Fellow, Canadian Institute for Advanced Research, Toronto, Ontario M5G 1Z8, Canada*

(Dated: January 4, 2018)

Quantum simulations are bound to be one of the main applications of near-term quantum computers. Quantum chemistry and condensed matter physics are expected to benefit from these technological developments. Several quantum simulation methods are known to prepare a state on a quantum computer and measure the desired observables. The most resource economic procedure is the variational quantum eigensolver (VQE), which has traditionally employed unitary coupled cluster as the ansatz to approximate ground states of many-body fermionic Hamiltonians. A significant caveat of the method is that the initial state of the procedure is a single reference product state with no entanglement extracted from a classical Hartree-Fock calculation. In this work, we propose to improve the method by initializing the algorithm with a more general fermionic Gaussian state, an idea borrowed from the field of nuclear physics. We show how this Gaussian reference state can be prepared with a linear-depth circuit of quantum matchgates. By augmenting the set of available gates with nearest-neighbor phase coupling, we generate a low-depth circuit ansatz that can accurately prepare the ground state of correlated fermionic systems. This extends the range of applicability of the VQE to systems with strong pairing correlations such as superconductors, atomic nuclei, and topological materials.

I. INTRODUCTION

The macroscopic properties of matter emerge from its microscopic quantum constituents whose massive components are mostly fermions. Understanding and modeling the behavior of a large number of interacting fermions is a central and fundamental problem in Physics and Chemistry which requires a large investment in computational resources as the memory required to represent a many-body state scales exponentially with the number of particles. Therefore, a computer operating on quantum mechanical principles have the potential to revolutionize the simulation of quantum systems [1, 2]. Such a machine would improve our ability to design new molecules such as drugs and catalysts [3], build new superconducting [4–6] and topological materials and improve our understanding of nuclear matter. Algorithm leveraging the advantages of quantum computers for quantum simulations have steadily been developed in the past two decades [4, 5, 7–20] as quantum processors are scaling in size [21–23]. Variational quantum eigensolvers (VQE) have recently appeared as a promising class of quantum algorithms designed to prepare states for quantum simulations [17, 24, 25]. However, near-term devices will suffer from limited coherence as a consequence of noise and finite experimental precision [26, 27]. This incentives the search for low-depth circuits for quantum simulations and state preparation [28, 29].

In this paper, we present a new type of low-depth VQE ansatz motivated by the Bogoliubov coupled cluster theory [30–32]. Our approach can be used to prepare the ground state of correlated fermions with pairing interactions by systematically appending variational cycles com-

posed of linear-depth blocks of 2-qubit gates. In section II, we first review the formulation of the strong correlation problem for fermions in the context of second quantization. We then present the unitary version of Bogoliubov coupled cluster theory and review how the generalized Hartree-Fock (GHF) reference state can be computed as a fermionic Gaussian state. Using the theory of matchgates, we show how pure fermionic Gaussian states can be exactly prepared on a quantum computer using a linear-depth circuit. Finally, we introduce the low-depth circuit ansatz (LDCA), consisting of the previous matchgate circuit plus additional nearest-neighbor phase coupling. We numerically benchmark the LDCA in section III for the prototypical examples of the Fermi-Hubbard model in condensed matter and the automerization reaction of cyclobutadiene in quantum chemistry, showing its potential to describe the exact ground state of strongly correlated systems.

II. GENERALIZED VARIATIONAL QUANTUM EIGENSOLVER

In this section, we review and extend the theoretical foundations of VQE. Specifically, in subsection II A, we review the definition of finding the ground state of fermionic Hamiltonians as found in quantum chemistry, condensed matter, and nuclear physics. In subsection II B we introduce the Bogoliubov unitary coupled cluster (BUCC) theory as a variational ansatz to the ground state problem. In subsection II C we review the formalism of the GHF theory as this is the starting point of the BUCC optimization method as well as the new

method presented in the following subsection. In subsection IID we show how a GHF state can be prepared on a quantum processor using matchgates and introduce a LDCA which can be used to prepare the ground state of fermionic Hamiltonian with surprisingly high accuracy. Finally, in subsection IIE, we outline an implementation to compute the analytical gradient of the LDCA using quantum resources.

A. Formulation of the problem

Many systems in quantum chemistry [33], condensed matter [34–36], and nuclear structure physics [37, 38] can be modeled by an ensemble of interacting fermions (electrons, nucleons) described by a second quantized Hamiltonian of the form

$$\begin{aligned} H = & \sum_{pq} (t_{pq} a_p^\dagger a_q + \Delta_{pq} a_p^\dagger a_q^\dagger + \Delta_{pq}^* a_q a_p) \\ & + \sum_{pqrs} v_{pqrs} a_p^\dagger a_q^\dagger a_s a_r \\ & + \sum_{pqrst} w_{pqrst} a_p^\dagger a_q^\dagger a_r^\dagger a_u a_t a_s. \end{aligned} \quad (1)$$

In general, the p, q, \dots, u indices run over all relevant quantum numbers (e.g. position, momentum, band number, spin, angular momentum, isospin, etc) which define M fermionic modes. The fermionic mode operators follow canonical anti-commutation relations $\{a_k, a_l^\dagger\} = \delta_{kl}$ and $\{a_k, a_l\} = \{a_k^\dagger, a_l^\dagger\} = 0$. The kinetic energy terms t_{pq} and the interaction v_{pqrs} are ubiquitous in most theories, while pairing terms Δ_{pq} often appear in the context of mean-field superconductivity, and the three-body interaction term w_{pqrst} can be phenomenologically introduced in nuclear physics [39].

As a prerequisite to calculating various observable quantities, we are interested in finding the ground state $\rho_0 = |\Psi_0\rangle\langle\Psi_0|$ of the Hamiltonian (1) such that the energy E is minimized over the set of all possible states ρ in a given Hilbert space:

$$\begin{aligned} E_0 & \equiv E(\rho_0) \\ & = \min_{\rho} E(\rho) \\ & = \min_{\rho} \text{tr}(H\rho). \end{aligned} \quad (2)$$

When this minimization cannot be done either analytically or with numerically exact methods, we have to resort to approximate methods such as variational ansatzes. One such ansatz, the BUCC method, is defined in the next subsection.

B. Bogoliubov unitary coupled cluster theory

Coupled cluster methods are used in ab initio quantum chemistry calculations to describe correlated many-

body states with a better accuracy than the Hartree-Fock method. Bogoliubov- and quasiparticle-based coupled cluster methods extends the range of applicability of those methods to systems with mean-field paired states [30–32]. Anticipating the implementation on quantum computers, we present the formalism for the unitary version of the Bogoliubov coupled cluster theory. We first review the Bogoliubov transformation and the parametrization of the ansatz.

The most general linear transformation acting on fermionic creation and annihilation operators that preserves the canonical anti-commutation relation is the Bogoliubov transformation. In this transformation, the quasiparticle operators $(\beta_{p'}^\dagger; \beta_{p'})$ are related to the single-particle operators $(a_p^\dagger; a_p)$ by a unitary matrix

$$\begin{aligned} \beta_{p'}^\dagger & = \sum_p (U_{pp'} a_p^\dagger + V_{pp'} a_p) \\ \beta_{p'} & = \sum_p (U_{pp'}^* a_p + V_{pp'}^* a_p^\dagger). \end{aligned} \quad (3)$$

This transformation preserves the canonical anti-commutation relation such that $\{\beta_k, \beta_l^\dagger\} = \delta_{kl}$ and $\{\beta_k, \beta_l\} = \{\beta_k^\dagger, \beta_l^\dagger\} = 0$. By introducing the vector notation $\vec{a}^\top = (a_1, \dots, a_M, a_1^\dagger, \dots, a_M^\dagger)$ and $\vec{\beta}^\top = (\beta_1, \dots, \beta_M, \beta_1^\dagger, \dots, \beta_M^\dagger)$, it is easy to express (3) in matrix notation as $\vec{\beta} = \mathcal{U}\vec{a}$ where the Bogoliubov transformation is unitary $\mathcal{U}^{-1} = \mathcal{U}^\dagger$ and its matrix is defined as

$$\mathcal{U} = \begin{pmatrix} \mathbf{U}^* & \mathbf{V}^* \\ \mathbf{V} & \mathbf{U} \end{pmatrix}. \quad (4)$$

The ground state of a quadratic Hamiltonian (all $v_{pqrs} = 0$ and $w_{pqrst} = 0$) is a product state

$$|\Phi_0\rangle = C \prod_{k=1}^M \beta_k |\text{vac}\rangle, \quad (5)$$

where $|\text{vac}\rangle$ is the Fock vacuum and C is a normalization factor. If the ground state is not degenerate, (5) acts as a quasiparticle vacuum $\beta_j |\Phi_0\rangle = 0$.

We can define the quasiparticle cluster operator $\mathcal{T} = \mathcal{T}_1 + \mathcal{T}_2 + \mathcal{T}_3 + \dots$ where

$$\begin{aligned} \mathcal{T}_1 & = \sum_{k_1 k_2} \theta_{k_1 k_2} \beta_{k_1}^\dagger \beta_{k_2}^\dagger \\ \mathcal{T}_2 & = \sum_{k_1 k_2 k_3 k_4} \theta_{k_1 k_2 k_3 k_4} \beta_{k_1}^\dagger \beta_{k_2}^\dagger \beta_{k_3}^\dagger \beta_{k_4}^\dagger \\ \mathcal{T}_3 & = \sum_{k_1 k_2 k_3 k_4 k_5 k_6} \theta_{k_1 k_2 k_3 k_4 k_5 k_6} \beta_{k_1}^\dagger \beta_{k_2}^\dagger \beta_{k_3}^\dagger \beta_{k_4}^\dagger \beta_{k_5}^\dagger \beta_{k_6}^\dagger. \end{aligned} \quad (6)$$

The $\theta_{k_1 k_2 \dots} \in \mathbb{C}$ are variational parameters which are fully antisymmetric such that $\theta_{k_1 k_2 \dots} = (-1)^{\xi(P)} \theta_{P(k_1 k_2 \dots)}$, where $\xi(P)$ is the signature of the permutation P . The BUCC ansatz is defined as

$$|\Psi(\Theta)\rangle = e^{i(\mathcal{T}(\Theta) + \mathcal{T}^\dagger(\Theta))} |\Phi_0\rangle. \quad (7)$$

where Θ corresponds to the set of variational parameters $\theta_{k_1 k_2 \dots}$ and $|\Phi_0\rangle$ is a reference state. Since the transformation is unitary $|\langle \Psi(\Theta) | \Psi(\Theta) \rangle| = 1$, $|\Psi(\Theta)\rangle$ is always normalized. The BUCC ansatz is said to be over single (BUCCS) or double excitations (BUCCSD) if the cluster operator \mathcal{T} is truncated at the first or second order.

To variationally optimize the BUCC ansatz, we aim to find the angles Θ that minimize the energy

$$\min_{\Theta} E(\Theta) = \langle \Psi(\Theta) | H | \Psi(\Theta) \rangle \quad (8)$$

subject to the constraint that the number of particles

$$\begin{aligned} \langle N(\Theta) \rangle &= \langle \Psi(\Theta) | N | \Psi(\Theta) \rangle \\ &= \sum_{p=1}^M \langle \Psi(\Theta) | a_p^\dagger a_p | \Psi(\Theta) \rangle \end{aligned} \quad (9)$$

should be kept constant, as the quasiparticles operators generally do not preserve the total particle number. In the next subsection we will explicitly show how to compute the reference state from the generalized Hartree-Fock theory before describing the details of the implementation of the quantum algorithm.

C. Generalized Hartree-Fock theory

Here we show how to obtain the Bogoliubov matrix (4) used to define the reference state (5). The method relies on the theory of fermionic Gaussian states [40, 41] for which we review the formalism and a method to obtain the covariance matrix of the ground state without a self-consistent loop. Fermionic Gaussian states are a useful starting point for quantum simulations as they include the family of Slater determinants from Hartree-Fock theory and Bardeen-Cooper-Schrieffer (BCS) states found in the mean-field theory of superconductivity [42, 43] and can be easily prepared on a quantum computer [44].

For M fermionic modes, it is convenient to define the $2M$ Majorana operators

$$\begin{aligned} \gamma_j &= \gamma_j^A = a_j^\dagger + a_j \\ \gamma_{j+M} &= \gamma_j^B = -i(a_j^\dagger - a_j) \end{aligned} \quad (10)$$

as the fermionic analogues of position and momentum operators. Let's note that we used either the extended index notation (from 1 to $2M$) or the A, B superscript notation interchangeably throughout the paper to make the equations clearer. Their commutation relation satisfies $\{\gamma_k, \gamma_l\} = 2\delta_{kl}$ such that $\gamma_k^2 = 1$. It is useful to define the vector notation $\vec{\gamma}^\top = (\gamma_1, \dots, \gamma_M, \gamma_{M+1}, \dots, \gamma_{2M})$ and write $\vec{\gamma} = \Omega \vec{a}$ where

$$\Omega = \begin{pmatrix} \mathbf{1} & \mathbf{1} \\ i\mathbf{1} & -i\mathbf{1} \end{pmatrix}. \quad (11)$$

In this case, $\mathbf{1}$ is the $M \times M$ identity matrix. A general fermionic Gaussian state [40] has the form of the exponential of a quadratic product of fermionic operators

$$\rho = \frac{1}{Z} e^{-\frac{i}{4} \vec{\gamma}^\top G \vec{\gamma}}, \quad (12)$$

where Z is the normalization factor and G is a real and antisymmetric matrix such that $G^\top = -G$. It can be fully characterized by a real and antisymmetric covariance matrix which is defined by

$$\Gamma_{kl} = \frac{i}{2} \text{tr}(\rho [\gamma_k, \gamma_l]), \quad (13)$$

where $[\cdot, \cdot]$ is the commutator. For a pure Gaussian state, $\Gamma^2 = -\mathbf{1}$, where $\mathbf{1}$ is the $2M \times 2M$ identity matrix. In general, the purity is given by $\chi = -\frac{1}{2M} \text{tr}(\Gamma^2)$. In order to extract \mathcal{U} given a covariance matrix Γ , we make use of the complex covariance matrix representation

$$\Gamma_c = \frac{1}{4} \Omega^\dagger \Gamma \Omega^* = \begin{pmatrix} \mathbf{Q} & \mathbf{R} \\ \mathbf{R}^* & \mathbf{Q}^* \end{pmatrix}, \quad (14)$$

where $\mathbf{Q}_{kl} = \frac{i}{2} \langle [a_k, a_l] \rangle$ and $\mathbf{R}_{kl} = \frac{i}{2} \langle [a_k, a_l^\dagger] \rangle$ (expectation values are defined as $\langle O \rangle = \text{tr}(O\rho)$). From there, we can define the single-particle density operators $\kappa \equiv -i\mathbf{Q}$ and $\varrho \equiv \frac{1}{2}\mathbf{1} - i\mathbf{R}^\top$ and recast the Gaussian state in the form of a single-particle density matrix

$$\mathcal{M} = \begin{pmatrix} \varrho & \kappa^\dagger \\ \kappa & \mathbf{1} - \varrho^\top \end{pmatrix} \quad (15)$$

such that $\mathcal{M}^2 = \mathcal{M}$ for pure states [45]. If we define the matrix $\mathcal{E} = \begin{pmatrix} \mathbf{0} & \mathbf{0} \\ \mathbf{0} & \mathbf{1} \end{pmatrix}$, then it is possible to find the Bogoliubov transformation (4) with the eigenvalue equation

$$\mathcal{M}\mathcal{U}^\dagger = \mathcal{E}\mathcal{U}^\dagger. \quad (16)$$

Next, we show how to compute the covariance matrix (13) approximating the ground state of the Hamiltonian (1).

1. Finding the ground state

These steps are a review of the method found in [41] aimed at calculating the covariance matrix approximating the ground state of an interacting Hamiltonian without a self-consistent loop.

The Hamiltonian (1) can be rewritten with Majorana operators in the form

$$\begin{aligned} H &= i \sum_{pq} T_{pq} \gamma_p \gamma_q \\ &+ \sum_{pqrs} V_{pqrs} \gamma_p \gamma_q \gamma_r \gamma_s \\ &+ i \sum_{pqrst} W_{pqrst} \gamma_p \gamma_q \gamma_r \gamma_s \gamma_t \gamma_u \gamma_v \gamma_w \gamma_x \gamma_y \gamma_z \gamma_t \gamma_s, \end{aligned} \quad (17)$$

where $T^\top = -T$ and V and W are antisymmetric under the exchange of any two adjacent indices. Expectation values over gaussian states can be efficiently calculated using Wick's theorem which has the form

$$i^p \text{tr}(\rho \gamma_{j_1} \dots \gamma_{j_{2p}}) = \text{Pf}(\Gamma|_{j_1 \dots j_{2p}}), \quad (18)$$

where $1 \leq j_1 < \dots < j_{2p} \leq 2M$, $\Gamma|_{j_1 \dots j_{2p}}$ is the corresponding submatrix of Γ and

$$\begin{aligned} \text{Pf}(\Gamma) &= \frac{1}{2^M M!} \sum_{s \in S_{2M}} \text{sgn}(s) \prod_{j=1}^M \Gamma_{s(2j-1), s(2j)} \\ &= \sqrt{\det(\Gamma)} \end{aligned} \quad (19)$$

is the Pfaffian of a $2M \times 2M$ matrix defined from the symmetric group S_{2M} where $\text{sgn}(s)$ is the signature of the permutation s . Assuming that Wick's theorem holds, we can write an effective but state dependent quadratic Hamiltonian

$$h(\Gamma) = T + 6\text{tr}_B(V\Gamma) + 45\text{tr}_C(W\Gamma\Gamma), \quad (20)$$

where $\text{tr}_B(V\Gamma)_{ij} = \sum_{kl} V_{ijkl} \Gamma_{lk}$ and $\text{tr}_C(W\Gamma\Gamma)_{ij} = \sum_{klmn} W_{ijklmn} \Gamma_{kn} \Gamma_{ml}$. To get the covariance matrix of the reference state, we use the imaginary time evolution starting from a pure state $\Gamma(0)^2 = -\mathbf{1}$:

$$\Gamma(\tau) = O(\tau) \Gamma(0) O(\tau)^\top, \quad (21)$$

where the orthogonal time evolution operator is given by

$$O(\tau) = \mathbb{T} e^{2 \int_0^\tau d\tau' [h(\Gamma(\tau')), \Gamma(\tau')]}, \quad (22)$$

with \mathbb{T} being the time ordering. The steady state is reached when $[h(\Gamma), \Gamma] = 0$. This is guaranteed to lower the energy of an initial state and keep the purity of the initial $\Gamma(0)$ but the imaginary time evolution may get stuck in a local minimum. A second complementary approach consists in minimizing the free energy of (17). The procedure simply involves fixed point iterations on the transcendental equation

$$\Gamma = \lim_{\beta \rightarrow \infty} \tanh[2i\beta h(\Gamma)]. \quad (23)$$

In our numerical experiments, we find that an imaginary time evolution (21) followed by a fixed point evolution (23) is numerically stable and consistently reaches the desired GHF ground state. In the following subsection, we will show how the theory of matchgates can be used to prepare a pure Gaussian state on a quantum computer as a reference state for a variational procedure.

D. The quantum subroutine

It is expected that quantum computer will enable the simulation of quantum systems beyond the reach of classical computers. An important challenge for practical

simulations is to prepare the ground state of interesting Hamiltonians with high accuracy. The VQE protocol [14, 17, 24, 25, 28] suggests a general procedure to reach this ground state. However, current implementations of the protocol have to trade long circuit depth for accuracy in a non-controllable manner. In this subsection, we introduce a composable VQE ansatz which is both accurate and hardware efficient with the added advantage of being able to represent states with BCS-like pairing correlations. Our method relies on the theory of matchgates and its relation to fermionic linear optics [44, 46–50] to both prepare a reference Gaussian state and parametrize an ansatz with a transformation analogous to fermionic non-linear optics. After a brief review of the theory of matchgates, we show how a given pure Gaussian state can be prepared on a quantum register with a linear-depth algorithm. A different algorithm with the same scaling was recently proposed in [51]. Unlike the procedure in [51], that relies on a gate decomposition strategy, our method has a fixed circuit structure with variable parameters. We then proceed to introduce a low-depth circuit ansatz with inherited properties of the BUCC ansatz and the apparent accuracy of the full configuration interaction method.

1. Matchgate decomposition of a Bogoliubov transformation

In the computational basis of a 2-qubit Hilbert space, matchgates [46] have the general form

$$\mathcal{G}(A, B) = \begin{pmatrix} p & 0 & 0 & q \\ 0 & w & x & 0 \\ 0 & y & z & 0 \\ r & 0 & 0 & s \end{pmatrix}, \quad (24)$$

where $A = \begin{pmatrix} p & q \\ r & s \end{pmatrix}$ and $B = \begin{pmatrix} w & x \\ y & z \end{pmatrix}$ are $SU(2)$ matrices with the same determinant $\det A = \det B$. They form a group which is generated by the tensor product of nearest-neighbor Pauli operators

$$\begin{aligned} \sigma_x^j \otimes \sigma_x^{j+1} &= -i\gamma_j^B \gamma_{j+1}^A \\ \sigma_x^j \otimes \sigma_y^{j+1} &= -i\gamma_j^B \gamma_{j+1}^B \\ \sigma_y^j \otimes \sigma_x^{j+1} &= i\gamma_j^A \gamma_{j+1}^A \\ \sigma_y^j \otimes \sigma_y^{j+1} &= i\gamma_j^A \gamma_{j+1}^B \\ \sigma_z^j \otimes \mathbb{I}^{j+1} &= -i\gamma_j^A \gamma_j^B \\ \mathbb{I}^j \otimes \sigma_z^{j+1} &= -i\gamma_{j+1}^A \gamma_{j+1}^B, \end{aligned} \quad (25)$$

which also correspond to the Jordan-Wigner transformed product of all products of nearest-neighbor Majorana operators, therefore establishing the connection with fermionic gaussian operations. The Bogoliubov transformation (3) can be written as an $SO(2M)$ transformation

of the Majorana operators (10) as $\vec{\gamma}' = \mathcal{R}\vec{\gamma}$, where

$$\mathcal{R} = \begin{pmatrix} \text{Re}(\mathbf{U} + \mathbf{V}) & -\text{Im}(\mathbf{U} - \mathbf{V}) \\ \text{Im}(\mathbf{U} + \mathbf{V}) & \text{Re}(\mathbf{U} - \mathbf{V}) \end{pmatrix}. \quad (26)$$

To implement this transformation on a quantum processor, there exists a quantum circuit of nearest-neighbor matchgates U_{Bog} acting on M qubits [49] such that

$$U_{\text{Bog}} \gamma_j U_{\text{Bog}}^\dagger = \sum_{k=1}^{2M} \mathcal{R}_{kj} \gamma_k. \quad (27)$$

An example of such a circuit known as the fermionic fast Fourier transform is described in [44]. In general, the Hoffman algorithm [52] can be used to decompose U_{Bog} in $2M(M-1)$ $SO(4)$ rotations between pairs of modes and M $SO(2)$ local phases. In total, these $2M^2 - M$ angles correspond to the same number of quantum gates. Using the fact that quantum gates can be operated in parallel in a linear chain of qubits, any transformation \mathcal{R} can be implemented in circuit depth $8 \lceil \frac{M}{2} \rceil + 1$, as detailed in Figure 1.

Since the Hoffman method assumes sequential operations on each pair of modes, we used an optimal control scheme [53, 54] in $SO(2M)$ to allow an easy parametrization of gates acting in parallel. This is generally efficient on a classical computer since the matchgates only operate on a much smaller subspace of the full $SU(2^M)$ transformation allowed on M qubits. The transformation \mathcal{R} can be decomposed in local and nearest-neighbor mode rotations such that

$$\begin{aligned} \mathcal{R} &= \prod_{k=1}^{\lceil \frac{M}{2} \rceil} \left\{ \prod_{\mu, \nu} \prod_{j \in \text{odd}} r_{j,j+1}^{\mu\nu} \left(\theta_{j,j+1}^{\mu\nu(k)} \right) \right. \\ &\quad \times \left. \prod_{\mu, \nu} \prod_{j \in \text{even}} r_{j,j+1}^{\mu\nu} \left(\theta_{j,j+1}^{\mu\nu(k)} \right) \right\} \\ &\quad \times \prod_{j=1}^M r_{jj}^{AB} \left(\theta_{jj}^{AB} \right), \end{aligned} \quad (28)$$

where $\mu, \nu \in \{A, B\}$ and $j \in \{1, \dots, M\}$. The mode rotations are parametrized by the $2M^2 - M$ angles $\theta_{ij}^{\mu\nu(k)}$

$$r_{ij}^{\mu\nu} = e^{2\theta_{ij}^{\mu\nu} h_{ij}^{\mu\nu}} \quad (29)$$

with $SO(2M)$ Hamiltonians

$$h_{ij}^{\mu\nu} = \delta_{i\mu, j\nu} - \delta_{j\nu, i\mu}. \quad (30)$$

The optimal control method maximizes the fidelity function

$$\Phi = \frac{1}{2M} \text{tr} \{ \mathcal{R}_{\text{target}}^\top \mathcal{R}(\Theta) \} \quad (31)$$

using the gradient

$$\frac{\partial r_{ij}^{\mu\nu}}{\partial \theta_{kl}^{\alpha\beta}} = 2h_{ij}^{\mu\nu} r_{ij}^{\mu\nu} \delta_{\alpha\mu} \delta_{\beta\nu} \delta_{ki} \delta_{lj}. \quad (32)$$

As shown in Figure 1 on a 8-qubit example, this decomposition explicitly translates into a quantum circuit of single qubit phase-rotations

$$R_j^Z = e^{i\theta_{ii}^{AB} \sigma_z^i} \quad (33)$$

and nearest-neighbor matchgates

$$G_{ij}^{(k)} = R_{ij}^{XX(k)} R_{ij}^{-YY(k)} R_{ij}^{XY(k)} R_{ij}^{-YX(k)}, \quad (34)$$

where each rotation corresponds to

$$\begin{aligned} R_{ij}^{-YX(k)} &= e^{-i\theta_{ij}^{AA(k)} \sigma_y^i \otimes \sigma_x^j} \\ R_{ij}^{XY(k)} &= e^{i\theta_{ij}^{BB(k)} \sigma_x^i \otimes \sigma_y^j} \\ R_{ij}^{-YY(k)} &= e^{-i\theta_{ij}^{AB(k)} \sigma_y^i \otimes \sigma_y^j} \\ R_{ij}^{XX(k)} &= e^{i\theta_{ij}^{BA(k)} \sigma_x^i \otimes \sigma_x^j}. \end{aligned} \quad (35)$$

Each parallel cycle interleaves gates between even and odd nearest neighbors

$$U_{\text{MG}}^{(k)} = \prod_{i \in \text{odd}} G_{i,i+1}^{(k)} \prod_{i \in \text{even}} G_{i,i+1}^{(k)} \quad (36)$$

and there are $\lceil \frac{M}{2} \rceil$ cycles in total:

$$U_{\text{MG}}^{\text{NN}} = \prod_{k=1}^{\lceil \frac{M}{2} \rceil} U_{\text{MG}}^{(k)}. \quad (37)$$

Finally, the unitary Bogoliubov transformation can be composed as

$$U_{\text{Bog}} = U_{\text{MG}}^{\text{NN}} \prod_{i=1}^M R_i^Z \quad (38)$$

and is also a gaussian operation of the form $U_{\text{Bog}} = e^{i \sum_{pq} \tau_{pq} \gamma_p \gamma_q}$, where $\tau^\top = -\tau$. In the case where the reference state is a Slater determinant, only number-conserving matchgates are required to prepare the state and the depth of the circuit would scale as $4 \lceil \frac{M}{2} \rceil + 1$ (since all $\theta_{ij}^{AA(k)}$ and $\theta_{ij}^{BB(k)}$ are set to zero). It should be noticed that a unitary coupled cluster ansatz truncated at first order $e^{i(\mathcal{T}_1(\Theta) + \mathcal{T}_1^\dagger(\Theta))}$ is also a gaussian transformation and can be implemented in the same way as U_{Bog} with no trotterization. In what follows, we introduce a VQE scheme that builds on this observation by introducing non-matchgate variational terms into a gate sequence similar to the U_{Bog} decomposition.

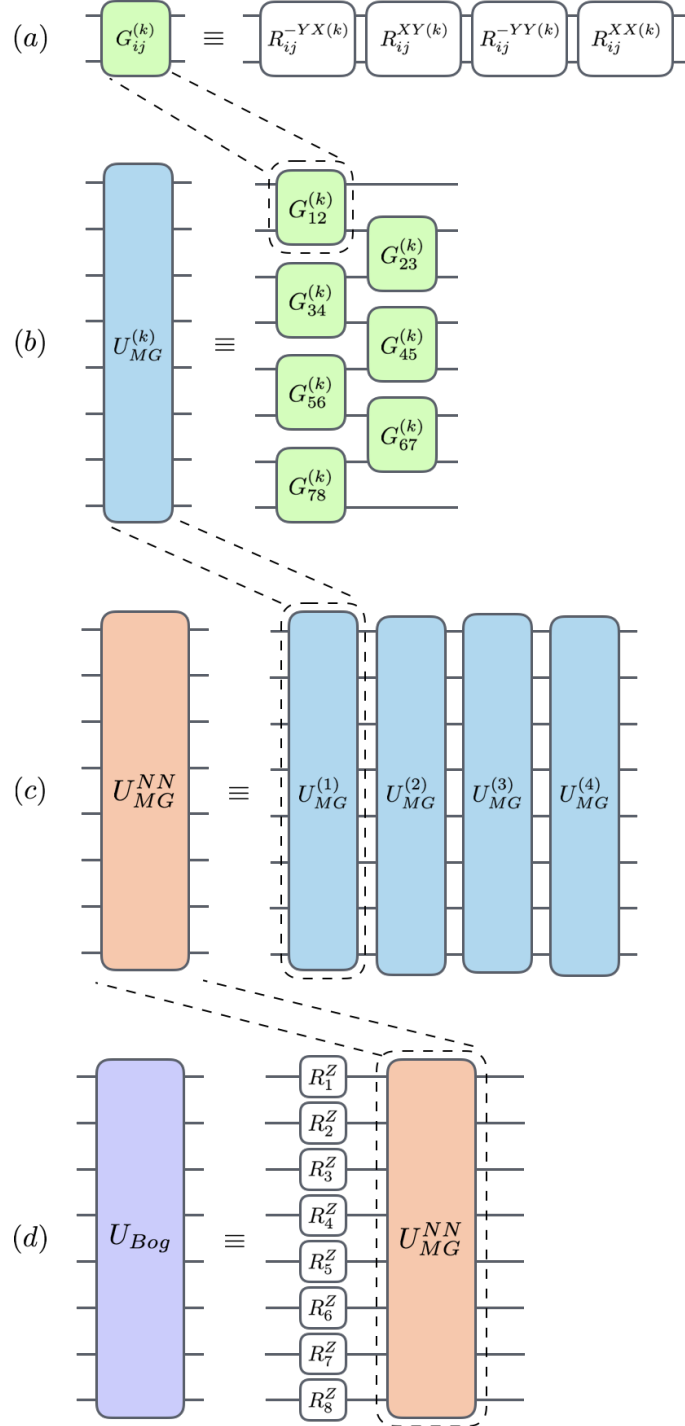


Figure 1. Example on 8 qubits of the decomposition of U_{Bog} in a circuit of local phase rotations and nearest-neighbor matchgates. In (a), each $G_{ij}^{(k)}$ is a 2-local operation between qubits i and j composed of 4 rotations for a layer k . As shown in (b), the unitary $U_{MG}^{(k)}$ for each layer k is built by operating $G_{ij}^{(k)}$'s in parallel first on the even pairs of qubits and then on the odd pairs. Then in (c), the complete sequence of nearest-neighbor matchgates U_{MG}^{NN} is composed by a sequence of $\lceil \frac{M}{2} \rceil$ layers. In (d), single qubit phase rotations R_j^Z are used to complete the U_{Bog} circuit.

2. A low-depth circuit ansatz

The Bogoliubov transformation (38) acts as a change of basis of the fermionic modes. Therefore, one can simply follow the VQE protocol [14] to implement the BUCC ansatz (7) and measure the expectation values $\langle \tilde{H} \rangle = \langle U_{\text{Bog}} H U_{\text{Bog}}^\dagger \rangle$ and $\langle \tilde{N} \rangle = \langle U_{\text{Bog}} N U_{\text{Bog}}^\dagger \rangle$ in the modified basis to prepare an approximate ground state of (1). This has the advantage of extending the range of Hamiltonians that can be processed to those with non-number conserving terms (like pairing fields) when compared to the traditional unitary coupled cluster ansatz. However, the change of basis may significantly increase the number of terms that have to be measured. In order to reduce the number of measurements in the VQE protocol, one can start in the product state (5) and carry out the variational unitary (7) in the quasiparticle basis, followed by an inverse Bogoliubov transformation using matchgates and measurement of the expectation values of the Hamiltonian (1) and the number operator N in the original fermionic orbital basis. In the quasiparticle basis, we can map the Bogoliubov operators to qubit operators with the Jordan-Wigner transformation [7, 55, 56] since they follow the canonical anti-commutation relation

$$\beta_p^\dagger = (-1)^{p-1} \left(\bigotimes_{j=1}^{p-1} \sigma_z \right) \otimes \sigma_+ \quad (39)$$

$$\beta_p = (-1)^{p-1} \left(\bigotimes_{j=1}^{p-1} \sigma_z \right) \otimes \sigma_-$$

and use the same mapping for Fermionic operators a_p^\dagger and a_p after the Bogoliubov transformation. Still, assuming that the number of fermionic particles is proportional to the number of orbitals, a major caveat of BUCCSD-like schemes is that the number of variational parameters will scale as $O(M^4)$. In the Jordan-Wigner picture, these terms can be implemented with $O(M^6)$ gates [57, 58]. It is expected that near-term quantum processor will continue to suffer from error rates that make this type of scaling impractical, and therefore more hardware-efficient VQE schemes must be sought [28].

Given that the gate decomposition of U_{Bog} can also exactly parametrize a BUCCS VQE protocol in linear circuit depth, we propose using a scheme augmented with nearest-neighbor phase coupling $\sigma_z \otimes \sigma_z$ rotations to mimic the effects of the quartic variational terms of \mathcal{T}_2 . Related ideas have already been explored in efficient classical non-gaussian variational methods with great success [59]. In a loose sense, our scheme is a parametrized fermionic non-linear optics circuit that does not involve any trotterization of the variational terms. The algorithm is illustrated in Figure 2. As a first step, the quasiparticle vacuum (5) is prepared in the Bogoliubov picture with $X = \begin{pmatrix} 0 & 1 \\ 1 & 0 \end{pmatrix}$ gates acting on each qubits to yield the state $|1\rangle^{\otimes M}$ in the computational basis. In what follows, we will define a L -cycle ansatz built from nearest-neighbor variational matchgates augmented with $\sigma_z \otimes \sigma_z$

rotations. The measurement of the expectation values can be done in the original basis by applying the inverse Bogoliubov transformation U_{Bog}^\dagger defined previously.

In a cycle l of the low-depth circuit ansatz (LDCA), the nearest-neighbor matchgates (34) are replaced by

$$K_{ij}^{(k,l)} \left(\Theta_{i,j}^{(k,l)} \right) = R_{ij}^{XX(k,l)} R_{ij}^{-YY(k,l)} \times R_{ij}^{ZZ(k,l)} R_{ij}^{XY(k,l)} R_{ij}^{-YX(k,l)}, \quad (40)$$

where the rotations are defined as

$$\begin{aligned} R_{ij}^{-YX(k,l)} &= e^{-i\theta_{ij}^{-YX(k,l)} \sigma_y^i \otimes \sigma_x^j} \\ R_{ij}^{XY(k,l)} &= e^{i\theta_{ij}^{XY(k,l)} \sigma_x^i \otimes \sigma_y^j} \\ R_{ij}^{ZZ(k,l)} &= e^{i\theta_{ij}^{ZZ(k,l)} \sigma_z^i \otimes \sigma_z^j} \\ R_{ij}^{-YY(k,l)} &= e^{-i\theta_{ij}^{-YY(k,l)} \sigma_y^i \otimes \sigma_y^j} \\ R_{ij}^{XX(k,l)} &= e^{i\theta_{ij}^{XX(k,l)} \sigma_x^i \otimes \sigma_x^j}. \end{aligned} \quad (41)$$

Each layer k applies those variational rotations in parallel first on the even pairs and then on the odd pairs such that

$$U_{\text{VarMG}}^{(k,l)} \left(\Theta^{(k,l)} \right) = \prod_{i \in \text{odd}} K_{i,i+1}^{(k,l)} \left(\Theta_{i,i+1}^{(k,l)} \right) \times \prod_{i \in \text{even}} K_{i,i+1}^{(k,l)} \left(\Theta_{i,i+1}^{(k,l)} \right). \quad (42)$$

A cycle l is composed of $\lceil \frac{M}{2} \rceil$ layers such that the variational ansatz is equivalent to a BUCCS transformation when the $\theta_{ij}^{ZZ(k,l)}$ are equal to zero:

$$U_{\text{VarMG}}^{\text{NN}(l)} \left(\Theta^{(l)} \right) = \prod_{k=1}^{\lceil \frac{M}{2} \rceil} U_{\text{VarMG}}^{(k,l)} \left(\Theta^{(k,l)} \right). \quad (43)$$

Finally, the L cycle are assembled sequentially to form the complete variational ansatz

$$U_{\text{VarMG}}(\Theta) = \prod_{l=1}^L U_{\text{VarMG}}^{\text{NN}(l)} \left(\Theta^{(l)} \right) \prod_{i=1}^M R_i^Z \left(\theta_i^Z \right), \quad (44)$$

with only one round of variational phase rotations

$$R_i^Z \left(\theta_i^Z \right) = e^{i\theta_i^Z \sigma_z^i}. \quad (45)$$

The variational state therefore has the form

$$|\Psi(\Theta)\rangle = U_{\text{Bog}}^\dagger U_{\text{VarMG}}(\Theta) \prod_{i=1}^M X_i |0\rangle^{\otimes M}, \quad (46)$$

where it can be noticed that the $L = 0$ case is simply equivalent to producing the GHF state. There are

5 variational angles per $K_{ij}^{(k,l)}$ and $M - 1$ of those terms per layer. Since each cycle has $\lceil \frac{M}{2} \rceil$ layers, a L -cycle circuit has $5L(M - 1)\lceil \frac{M}{2} \rceil + M$ variational angles, the extra term arising from the round of phase rotations. Since gates can be operated in parallel in a linear chain of qubits, the circuit depth is $(10L + 8)\lceil \frac{M}{2} \rceil + 4$ when we account for U_{Bog}^\dagger and the initial round of single-qubit X gates (this includes the final single-qubit rotations, $R_y(\frac{\pi}{2})$ or $R_x(-\frac{\pi}{2})$ gates (or equivalent), to measure the terms of the Hamiltonian in the form of Pauli strings). Therefore, this VQE scheme is hardware efficient in the sense that the circuit depth is linear in the number of qubits. The accuracy can also be systematically improved by increasing the number of cycles until either convergence is reached or errors dominate the precision of the result.

In the following section, we outline an implementation to compute the analytical gradient of the LDCA using quantum resources, which could be useful during the optimization procedure in VQE by guiding the search for the ground state and its energy.

E. Gradient Evaluation for LDCA

When optimizing the ansatz parameters to minimize the total energy, there may be a need to implement gradients depending on the selected optimization procedure. While direct search algorithms are generally more robust to noise than gradient-based approaches, they may require larger numbers of function evaluations [60]. On the other hand, numerical implementations of gradients rely heavily on the step size for accuracy. However, step sizes that are too small may lead to numerical instability and higher sampling cost. In addition, implementation of step sizes corresponding to desired accuracy are limited by experimental errors.

An alternative approach that exhibits high accuracy while maintaining reasonable computational cost may be to evaluate the gradient directly on the quantum computer given that the analytical form of the gradient is available. Here we employ a scheme similar to one outlined in [58] tailored to implement the analytical gradient of the LDCA unitary using an extra qubit and controlled two-qubit rotations. Recall the unitary for the complete variational ansatz shown in (44), which we called $U_{\text{VarMG}}(\Theta)$ parametrized by angles Θ . For this derivation, we will ignore the products of Z -rotations in the definition but computing the gradient with respect to these angles should be more straightforward. These initial Z -rotations are not as "nested" within the LDCA framework, so the gradient corresponding to one of such angles, say θ_j , simply involves inserting a controlled- Z gate following the unitary $\exp(-i\theta_j Z)$, to the circuit (where we use an ancilla qubit as the control qubit). Thus, we will instead focus on finding the gradients of the term $\prod_{l=1}^L U_{\text{VarMG}}^{NN}(\Theta^{(l)})$, which we will call $U'_{\text{VarMG}}(\Theta)$.

Consider the state $\Psi(\Theta)$, prepared by applying $U_{\text{VarMG}}(\Theta)$ to $|\Phi_0\rangle$, where $|\Phi_0\rangle$ corresponds to a reference state that does not depend on Θ . Here we wish to compute the derivative of the expectation value of the energy $E(\Theta) = \langle \Psi(\Theta) | H | \Psi(\Theta) \rangle$ with respect to each parameter in Θ . We will use the label $\theta_{j,n}^{(k,l)}$ for each parameter where j refers to the index of the qubit in the register, l to the circuit cycle, k to the circuit layer, and n to the appropriate Pauli string (in this case, $n \in \{-YX, XY, ZZ, -YY, XX\}$). Considering a Hamiltonian H that is independent of Θ , the derivative with respect to $\theta_{j,n}^{(k,l)}$ is given by

$$\frac{\partial E(\Theta)}{\partial \theta_{j,n}^{(k,l)}} = \langle \Phi_0 | U^\dagger H \frac{\partial U}{\partial \theta_{j,n}^{(k,l)}} | \Phi_0 \rangle + \langle \Phi_0 | \frac{\partial U^\dagger}{\partial \theta_{j,n}^{(k,l)}} H U | \Phi_0 \rangle \quad (47a)$$

$$= i \left(\langle \Phi_0 | U^\dagger H V_{j,n}^{(k,l)} | \Phi_0 \rangle - \langle \Phi_0 | V_{j,n}^{(k,l)\dagger} H U | \Phi_0 \rangle \right) \quad (47b)$$

$$= 2 \text{Im} \left(\langle \Phi_0 | V_{j,n}^{(k,l)\dagger} H U | \Phi_0 \rangle \right) \quad (47c)$$

where the operator $V_{j,n}^{(k,l)}(\Theta)$ is nearly identical to the unitary U'_{VarMG} except with a string of Pauli matrices $P_{j,n}^{k,l}$ inserted after the rotation term $R_{j,j+1}^{n(k,l)} = \exp(i\theta_{j,n}^{k,l} P_{j,n}^{k,l})$ included in the nearest-neighbor match-gate term $K_{j,j+1}^{(k,l)}$ and so on.

To compute the expectation value of the energy, we can employ the Hamiltonian averaging procedure [25, 61]. This involves measuring the expectation value of every term in the Hamiltonian and summing over them as shown in (48). Note that each term, which we call O_i , is a product of Pauli matrices obtained by performing the Jordan-Wigner or Bravyi-Kitaev transformation on the corresponding term in the second quantized Hamiltonian from (1).

$$E = \sum_i h_i \langle O_i \rangle. \quad (48)$$

Substituting (48) into (47c), the gradient can be expressed as:

$$\frac{\partial E(\Theta)}{\partial \theta_{j,n}^{(k,l)}} = 2 \sum_i h_i \text{Im} \left(\langle \Phi_0 | V_{j,n}^{(k,l)\dagger}(\Theta) O_i U(\Theta) | \Phi_0 \rangle \right) \quad (49)$$

Each of the terms in the sum above can be computed using the circuit shown in Figure 3. For a practical physical implementation of the analytical gradient, a circuit layout similar to one highlighted in [62] could be used, in which the control qubit of the gradient circuit is connected to all qubits in the register.

In the following section, we numerically benchmark the BUCC ansatz and LDCA on small instances of the Fermi-Hubbard model and the automerization reaction of cyclobutadiene, where we find that LDCA is able to prepare the exact ground state of those systems.

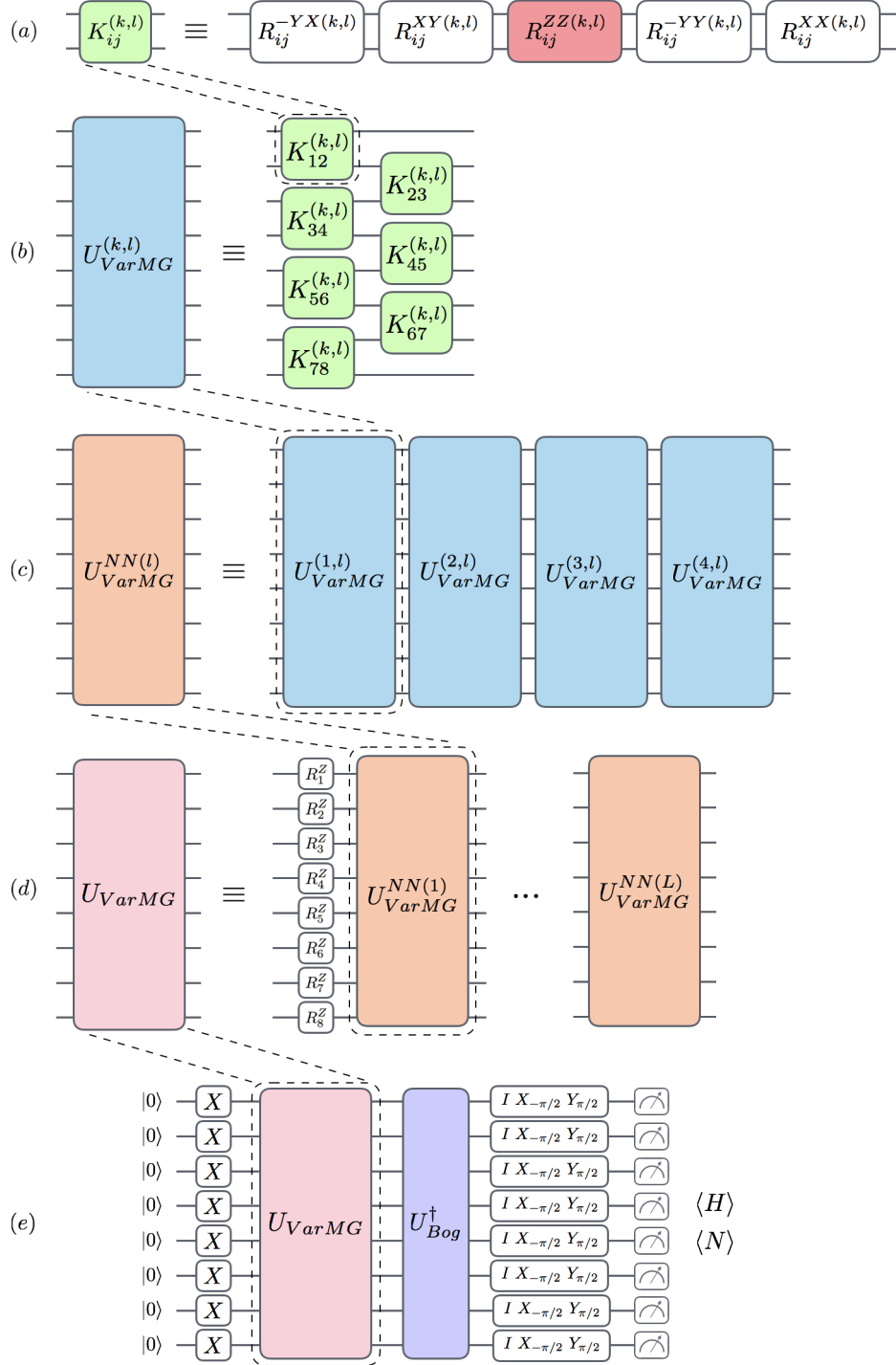


Figure 2. Gate decomposition of the L -cycle LDCA on a linear chain of 8 qubits. In (a), each $K_{ij}^{(k,l)}$ is a 2-local operation between qubits i and j composed of 5 rotations for a layer k . In (b), we build the unitary $U_{VarMG}^{(k,l)}$ for each layer k by applying $K_{ij}^{(k,l)}$'s in parallel first on the even pairs and then on the odd pairs. In (c), a cycle $U_{VarMG}^{NN(l)}$ is composed by a sequence of $\lceil \frac{M}{2} \rceil$ layers. In (d), we show the L -cycle construction of U_{VarMG} with one round of variational phase rotations. The full LDCA protocol is shown in (e) with the initial preparation of the quasiparticle vacuum and the transformation to the original fermionic basis U_{Bog}^\dagger .

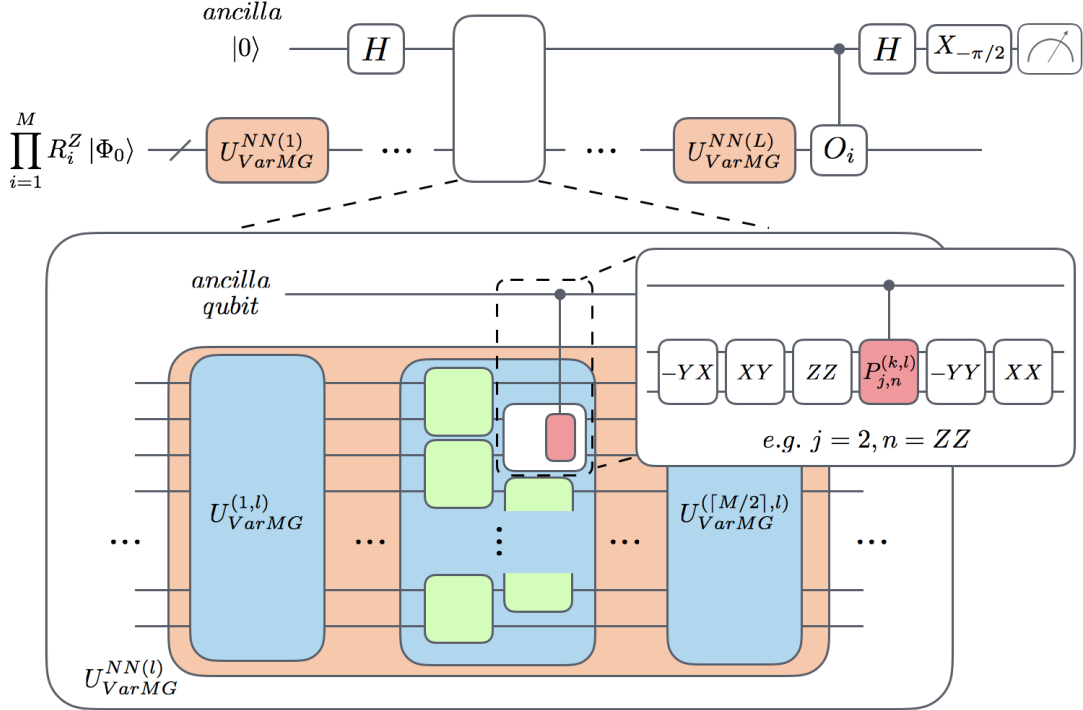


Figure 3. Circuit using an ancilla qubit to measure the imaginary component of $\langle \Phi_0 | V_{j,n}^{(k,l)\dagger} O_i U'_{VarMG} | \Phi_0 \rangle$ required to compute $\frac{\partial E(\Theta)}{\partial \theta_{j,n}^{(k,l)}}$. This figure illustrates an instance of the circuit where $j = 2$ and $n = ZZ$.

III. NUMERICAL EXAMPLES

In this section, we numerically test the performance of the previously described algorithms on instances of strongly correlated systems in condensed matter and quantum chemistry. Specifically, in subsection III A, we analyze the behavior of the ansatz on the Fermi-Hubbard model at half-filling at different interaction strengths. In subsection III B, we study the automerization reaction of cyclobutadiene modeled using the Pariser-Parr-Pople (PPP) Hamiltonian [63–65]. In both cases, the Hamiltonians are mapped to 8-qubit registers and we compare the energy and wavefunction accuracies for approximating the exact ground state for the following methods ansatzes: GHF, BUCCSD, and LDCA with 1 and 2 cycles.

In these cases, the state initialization has 8 single qubit X gates operated in parallel and the inverse Bogoliubov transformation has one layer of single qubit phase rotations and 112 nearest-neighbor matchgates. The state initialization and U_{Bog}^\dagger circuit add up to a circuit depth of 34. The LDCA method adds a layer of variational phase rotations and 140 nearest-neighbor gates per cy-

cle. Therefore 1-cycle LDCA adds 41 to the circuit depth (for a total of 75 with 148 variational parameters) and 2-cycle LDCA adds 81 to the circuit depth (for a total of 115 with 288 variational parameters).

For the numerical examples presented here, we find that 2-cycle LDCA is able to exactly recover the ground state of the simulated systems while 1-cycle LDCA performs better than the GHF solution but is not as accurate as BUCCSD. An important caveat is that the 2-cycle LDCA has more variational parameters (288) than the dimensions of the Hilbert space ($2^8 = 256$) but we still consider the result relevant for experimental implementations since the depth of the circuit is much shorter than what could be achieved with BUCC up to fourth order, which is required to recover the exact ground state of systems studied.

A. Fermi-Hubbard model

The Fermi-Hubbard model [66] is a prototypical example of correlated electrons. It is described by a tight-binding lattice of electrons interacting through a local

Coulomb force. The Hamiltonian is given by

$$\begin{aligned}
H^{\text{FH}} = & -t \sum_{\langle p,q \rangle} \sum_{\sigma=\uparrow,\downarrow} (a_{p\sigma}^\dagger a_{q\sigma} + a_{q\sigma}^\dagger a_{p\sigma}) \\
& -\mu \sum_p \sum_{\sigma=\uparrow,\downarrow} (n_{p\sigma} - \frac{1}{2}) \\
& +U \sum_p (n_{p\uparrow} - \frac{1}{2}) (n_{p\downarrow} - \frac{1}{2}),
\end{aligned} \tag{50}$$

where t is the kinetic energy between nearest-neighbor sites $\langle p,q \rangle$, U is the static Coulomb interaction and μ is the chemical potential. The number operator is $n_{p\sigma} = a_{p\sigma}^\dagger a_{p\sigma}$. While the one-dimensional Fermi-Hubbard model can be solved exactly with the Bethe ansatz [67, 68], the two-dimensional version can only be solved exactly for very specific values of the parameters and a general solution remains elusive. The phase diagram of the 2D model is known to be very rich and there are strong arguments that a better understanding of the model could yield the key to explain the physics of high-temperature cuprate superconductors [69–71].

Hybrid quantum-classical methods to systematically approximate the phase diagram of the Fermi-Hubbard model in the thermodynamical limit are known [6, 62] but they require preparing the ground state of a large cluster of the model with an accuracy that cannot be reached by previously proposed methods [5]. Here, we investigate the performance of the ansatz detailed in section II on an example of a 2×2 cluster of the Fermi-Hubbard model at half-filling ($\mu = 0$) that can be implemented on a 8-qubit quantum processor. As shown in figure 4, the GHF method performs well for small values of the interaction strength $\frac{U}{t}$ and exactly describes the tight-binding case where the Hamiltonian is quadratic. The BUCCSD ansatz offers a significant improvement over the GHF solution but fails to reach the exact ground state at strong interaction strengths. While 1-cycle LDCA offers an intermediate solution between GHF and BUCCSD, the 2-cycle LDCA solution performs surprisingly well as it is able to reach the exact ground state up to numerical accuracy for all values of the interaction strength. In all cases the preparation fidelity $|\langle \Psi(\Theta) | \Psi_0 \rangle|^2$ is directly correlated with the energy difference δE between the prepared state and the exact ground state $|\Psi_0\rangle$. We also show that all methods are able to handle Hamiltonians with pairing terms by introducing an artificial $\Delta \sum_i (a_{i\uparrow}^\dagger a_{i\downarrow}^\dagger + a_{i\downarrow} a_{i\uparrow})$. The accuracy of all methods improves with increasing $\frac{\Delta}{t}$ as the ground state gets closer to a fermionic Gaussian state.

We also tested a simpler one dimensional cluster of the Fermi-Hubbard model with 2 sites and found that it was possible to reach the exact ground state with both BUCCSD and the 1-cycle LDCA method for all values of the parameter U . This is expected for the BUCCSD method as this is equivalent to a full configuration interaction parametrization in this specific case. We do not have sufficient information to determine the number of cycles L required by LDCA to reach the ground state as a function of the cluster size since it would require

much more intense numerics. However, the fact that a 2×1 cluster requires only 1 cycle and that the 2×2 case reaches the ground state in 2 cycles leave open the possibility that the scaling is not an exponential function of the cluster size.

B. Cyclobutadiene

As an example of a quantum chemistry application, we studied the accuracy of the proposed methods in the description of cyclobutadiene automerization. The study of this reaction has been particularly challenging for theoretical chemists due to the strongly correlated character of the open-shell D_{4h} transition state in contrast with the weakly correlated character of the closed-shell D_{2h} ground state (${}^1A_{1g}$) [72]. An accurate theoretical treatment of the transition state would allow to confirm several observations about the mechanism, such as the alleged change in the aromatic character of the molecule between its ground and transition states as well as the involvement of a tunneling carbon atom in the reaction [72–75]. In addition, it would serve as a confirmation of the energy barrier for the automerization, for which experimental reports vary between 1.6 and 12.0 kcal/mol [76].

Although the Hamiltonian for cyclobutadiene can be obtained from a Hartree-Fock or a Complete Active Space (CAS) standard quantum chemistry calculation, we opted to describe the reaction using a Pariser-Parr-Pople (PPP) model Hamiltonian [63–65]. The PPP model captures the main physics of π -electron systems such as cyclobutadiene and also establishes a direct connection to the Fermi-Hubbard Hamiltonian studied in the previous section. Using this model, the Hamiltonian of cyclobutadiene can be written as

$$\begin{aligned}
H^{\text{PPP}} = & \sum_{i<j} t_{ij} E_{ij} \\
& + \sum_i U_i n_{i\alpha} n_{i\beta} + V_c \\
& + \frac{1}{2} \sum_{ij} \gamma_{ij} (n_{i\alpha} + n_{i\beta} - 1)(n_{j\alpha} + n_{j\beta} - 1),
\end{aligned} \tag{51}$$

where $E_{ij} = \sum_{\sigma=\alpha,\beta} a_{i\sigma}^\dagger a_{j\sigma} + a_{j\sigma}^\dagger a_{i\sigma}$, $n_{i\sigma} = a_{i\sigma}^\dagger a_{i\sigma}$, and the variables γ_{ij} are parameterized by the Mataga-Nishimoto formula [77]

$$\gamma_{ij}(r_{ij}) = \frac{1}{1/U + r_{ij}}. \tag{52}$$

The t_{ij} , U , and V_c parameters were obtained from [78, 79] as a function of the dimensionless reaction coordinate, λ , and the geometries of the ground as well as transition states were optimized at this level of theory.

Figure 5 compares the accuracies of different ansatzes for the cyclobutadiene automerization reaction. We observe that GHF ansatz is considerably improved by BUCCSD close to the D_{2h} ground state but the improve-

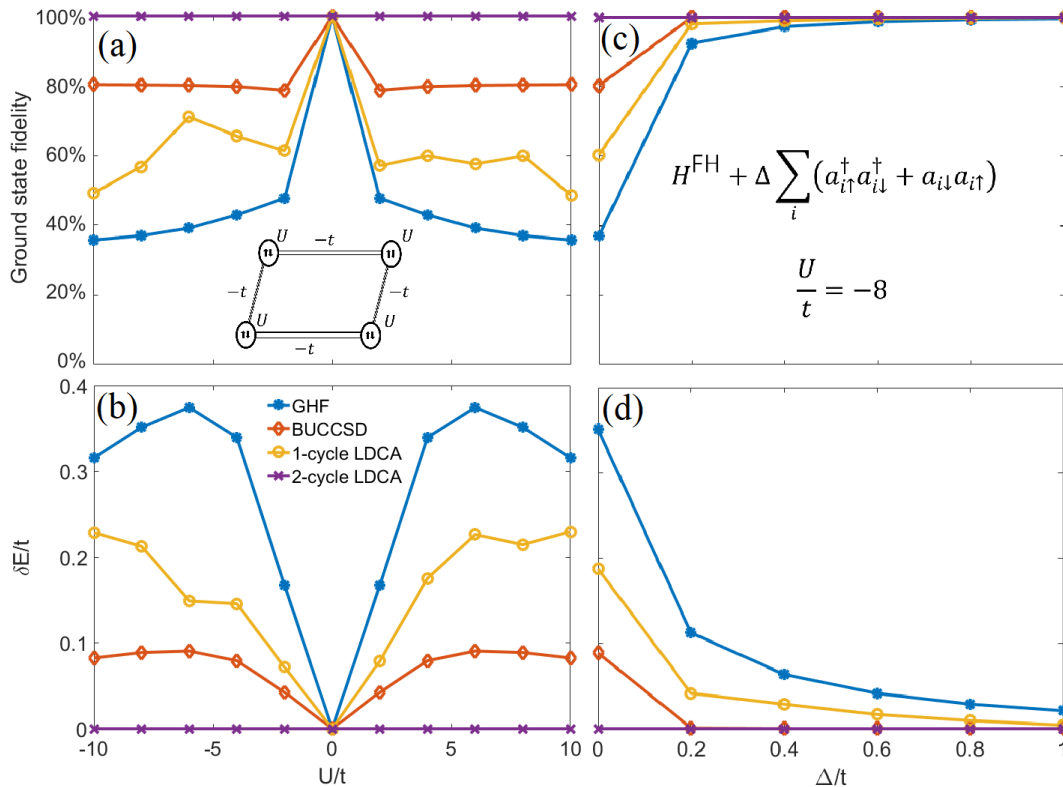


Figure 4. In (a), we show the fidelity of the ground state preparation of a 2×2 cluster of the Fermi-Hubbard model as a function of the interaction parameter U . The energy difference with the exact ground state with respect to the various methods is shown in (b). The energies are normalized by the hopping term t . In (c) and (d), we show respectively the fidelity and the energy difference in the case of an attractive cluster $\frac{U}{t} = -8$ with an additional s-wave pairing term Δ .

ment is less prominent as we approach the strongly correlated D_{4h} transition state. As in the 2×2 Fermi-Hubbard case, the 1-cycle LDCA method yields accuracies between those of GHF and BUCCSD while the 2-cycle LDCA method produces the numerically exact ground state for all values of λ . This surprising result suggests that LCDA is potentially useful for treating cases of strong correlation in quantum chemistry.

IV. DISCUSSION

The results presented in the previous section suggest that the LDCA could outperform other ansatzes employed for VQE calculations, such as BUCC, both in accuracy and efficiency. Being a method inspired by BUCC, the LDCA scheme inherits some properties of this ansatz. For instance, in the limit of 1-cycle LDCA with all $\theta_{ij}^{ZZ(k,1)}$ set to zero, we recover the BUCC ansatz with single excitations. We point out that this choice of parameters cannot improve the GHF solution since it only amounts to a basis rotation of the fermionic mode for which the Bogoliubov transformation has already been optimized. Since the mapping (35) between the Bogoli-

ubov transformation and the matchgate circuit relies on the Jordan-Wigner transformation which associates Pauli strings of length $O(M)$ to fermionic operators, it may be possible to further reduce the length of the measured Pauli strings by working out a similar mapping in the Bravyi-Kitaev basis [48] where operators are represented by strings of length $O(\log M)$. For completeness, we also numerically benchmarked the traditional UCCSD scheme [14, 25, 58] and found that it provides the same results as BUCCSD. This is expected in the case of Hamiltonians with no explicit pairing terms. However, such terms may appear in variational self-energy functional theory [6, 80–83] where fictitious pairing terms are added to a cluster Hamiltonian to recover the magnetic and superconducting phase diagram in the thermodynamic limit.

Regarding the number of variational parameters, LDCA scales as $O(LM^2)$ compared to $O(M^4)$ for UCCSD and BUCCSD with Gaussian basis set. There may exist constraints on the variational parameters of LDCA that reduce their total number. To explore whether it was possible to only measure $\langle H \rangle$ in the variational procedure, we tried the ansatz with only number conserving terms (such that all $\theta_{ij}^{XY(k,l)} = \theta_{ij}^{-YX(k,l)} = 0$) on the Fermi-Hubbard model but found a reduced overlap

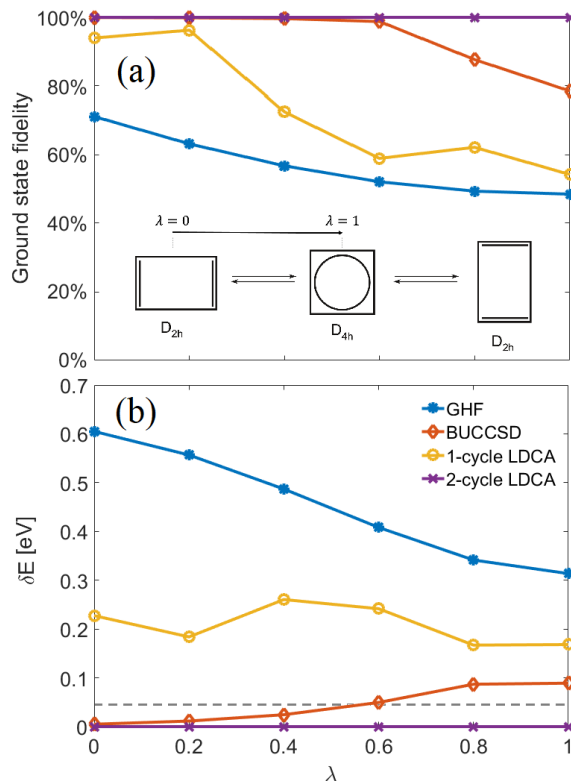


Figure 5. In (a), we show the fidelity of the ground state preparation along the automerization reaction path of cyclobutadiene. Subfigure (b) shows the difference with the exact ground state for the various ansatzes. Chemical accuracy is approximately 0.043 eV (dashed line).

with the exact ground state. This implies that a reconfiguration of the pairing amplitudes with respect to the GHF reference state is an important condition to reach an accurate ground state.

Our estimates of the circuit depth assume a quantum architecture consisting of a linear chain of qubits, which allows to maximize the parallel application of gates through the algorithm. We leave open the question of whether it is possible to achieve further improvements by using an architecture with increased connectivity. We also assumed that nearest-neighbor two-qubit gates could be implemented directly (as proposed for a linear chain of polar molecules [84]). Although this is not the case on current ion trap and superconducting circuit technologies, the required gates can be implemented as long as tunable nearest-neighbor entangling gates are available. In this case, only additional single-qubit basis rotation suffices, adding only a small overhead in circuit depth [85].

Due to its better accuracy and reduced scaling in depth and number of parameters compared to previous ansatzes, we believe that the LDCA approach is a feasible alternative for studying strongly correlated systems in near-term quantum devices. In this case, we propose

some strategies to ensure a better performance of the ansatz on real quantum processors with control inaccuracies. For instance, we could calibrate the angles $\theta_{ij}^{\mu\nu}$ of the gate sequence of U_{Bog}^\dagger by minimizing the difference between the values of $\langle H \rangle$ and $\langle N \rangle$ measured on the quantum computer and the values obtained numerically for the GHF reference state. Similarly, it should be possible to experimentally estimate the errors on the energy and the number of particles for a given L -cycle LDCA by comparing the values of $\langle H \rangle$ and $\langle N \rangle$ obtained with all $\theta_{ij}^{ZZ(k,1)}$ set to zero with the exact classical results computed as described in section II C. Instead of setting $\theta_{ij}^{ZZ(k,1)}$ to zero, one might also replace the ZZ rotations with equivalent time delays.

Finally, we point out that our formalism should be general enough to implement the simulation of nucleons [32]. However, we abstained from venturing in the numerical simulation of such systems as it is beyond our fields of expertise. Similarly, our method could be employed to study the ground state of gauge theories in the quantum link model [86–88].

V. CONCLUSION

In this work, we generalized the Bogoliubov coupled cluster ansatz to a unitary framework such that it can be implemented as a VQE scheme on a quantum computer. We showed how the required GHF reference state can be computed from the theory of fermionic Gaussian states. Those states include Slater determinants used in quantum chemistry as well as mean field superconducting BCS states. We described a procedure to prepare fermionic Gaussian states on a quantum computer using a circuit of nearest-neighbor matchgates with linear depth on the size of the system. By augmenting the set of available gates with nearest-neighbor $\sigma_z \otimes \sigma_z$ rotations, we constructed a low-depth circuit ansatz (LDCA) that can systematically improve the preparation of approximate ground states for fermionic Hamiltonians. Each added cycle increases linearly the depth of the quantum circuit, which makes it practical for implementations in near-term quantum devices.

We used a cluster of the Fermi-Hubbard model and the automerization of Cyclobutadiene as examples to assess the accuracy of the BUCC and LDCA ansatzes. Our results showed that LDCA has the potential to accurately describe the exact ground state of strongly correlated fermionic systems on a quantum processor. In addition, our proposed BUCC and LDCA approaches can be used to approximate the ground states of Hamiltonians with pairing fields. This feature, not present in previous ansatzes such as UCC, extends the range of applicability of VQE to problems in condensed matter and nuclear physics. Since the number of particles is not conserved in BUCC and LDCA, we must impose constraints on the number of particles to carry out the optimization in

the classical computer. Future work will be devoted to benchmarking the accuracy of the LDCA method for a larger variety of molecular systems and determining the scaling in the number of cycles required to describe the ground states of general systems.

ACKNOWLEDGMENTS

We would like to thank Ryan Babbush for helpful discussions. Jonathan Romero and Alán Aspuru-Guzik acknowledge the Air Force Office of Scientific Research for support under Award: FA9550-12-1-0046. Sukin Sim is supported by the DOE Computational Science Graduate Fellowship under grant number DE-FG02-97ER25308. Pierre-Luc Dallaire Demers and Alán Aspuru-Guzik acknowledge support from the Vannevar Bush Fellowship from the United States Department of Defense under award number N00014-16-1-2008 under the Office of Naval Research.

-
- [1] R. P. Feynman, *Int. J. Theor. Phys.* **21**, 467 (1982).
- [2] D. S. Abrams and S. Lloyd, *Phys. Rev. Lett.* **79**, 2586 (1997).
- [3] M. Reiher, N. Wiebe, K. M. Svore, D. Wecker, and M. Troyer, *Proceedings of the National Academy of Sciences* **114**, 7555 (2017).
- [4] B. Bauer, D. Wecker, A. J. Millis, M. B. Hastings, and M. Troyer, *Phys. Rev. X* **6** (2016), 10.1103/physrevx.6.031045.
- [5] D. Wecker, M. B. Hastings, N. Wiebe, B. K. Clark, C. Nayak, and M. Troyer, *Phys. Rev. A* **92**, 062318 (2015).
- [6] P.-L. Dallaire-Demers and F. K. Wilhelm, *Phys. Rev. A* **93**, 032303 (2016).
- [7] G. Ortiz, J. E. Gubernatis, E. Knill, and R. Laflamme, *Physical Review A* **64** (2001), 10.1103/physreva.64.022319.
- [8] A. Aspuru-Guzik, *Science* **309**, 1704 (2005).
- [9] I. Kassal, S. P. Jordan, P. J. Love, M. Mohseni, and A. Aspuru-Guzik, *Proceedings of the National Academy of Sciences* **105**, 18681 (2008).
- [10] J. D. Whitfield, J. Biamonte, and A. Aspuru-Guzik, *Molecular Physics* **109**, 735 (2011).
- [11] I. Kassal, J. D. Whitfield, A. Perdomo-Ortiz, M.-H. Yung, and A. Aspuru-Guzik, *Annu. Rev. Phys. Chem.* **62**, 185 (2011).
- [12] L. Veis, J. Višňák, T. Fleig, S. Knecht, T. Saue, L. Visscher, and J. Pittner, *Physical Review A* **85** (2012), 10.1103/physreva.85.030304.
- [13] U. L. Heras, A. Mezzacapo, L. Lamata, S. Filipp, A. Wallraff, and E. Solano, *Phys. Rev. Lett.* **112**, 200501 (2013).
- [14] A. Peruzzo, J. McClean, P. Shadbolt, M.-H. Yung, X.-Q. Zhou, P. J. Love, A. Aspuru-Guzik, and J. L. O’Brien, *Nat. Commun.* **5**, 4213 (2014).
- [15] R. Barends, L. Lamata, J. Kelly, L. Garcia-Alvarez, A. G. Fowler, A. Megrant, E. Jeffrey, T. C. White, D. Sank, J. Y. Mutus, B. Campbell, Y. Chen, Z. Chen, B. Chiaro, A. Dunsworth, I.-C. Hoi, C. Neill, P. J. J. O’Malley, C. Quintana, P. Roushan, A. Vainsencher, J. Wenner, E. Solano, and J. M. Martinis, *Nat. Commun.* **6**, 7654 (2015).
- [16] U. L. Heras, L. Garcia-Alvarez, A. Mezzacapo, E. Solano, and L. Lamata, *EPJ Quantum Technology* **2**, 8 (2015).
- [17] P. J. J. O’Malley, R. Babbush, I. D. Kivlichan, J. Romero, J. R. McClean, R. Barends, J. Kelly, P. Roushan, A. Tranter, N. Ding, B. Campbell, Y. Chen, Z. Chen, B. Chiaro, A. Dunsworth, A. G. Fowler, E. Jeffrey, A. Megrant, J. Y. Mutus, C. Neill, C. Quintana, D. Sank, A. Vainsencher, J. Wenner, T. C. White, P. V. Coveney, P. J. Love, H. Neven, A. Aspuru-Guzik, and J. M. Martinis, *Phys. Rev. X* **6** (2016), 10.1103/physrevx.6.031007.
- [18] D. Poulin, M. B. Hastings, D. Wecker, N. Wiebe, A. C. Doherty, and M. Troyer, *QIC* **15**, 361 (2015).
- [19] R. Babbush, D. W. Berry, I. D. Kivlichan, A. Y. Wei, P. J. Love, and A. Aspuru-Guzik, *New J. Phys.* **18**, 033032 (2016).
- [20] G. Zhu, Y. Subasi, J. D. Whitfield, and M. Hafezi, (2017), 1707.04760v1.
- [21] T. Monz, D. Nigg, E. A. Martinez, M. F. Brandl, P. Schindler, R. Rines, S. X. Wang, I. L. Chuang, and R. Blatt, *Science* **351**, 1068 (2016).
- [22] N. M. Linke, D. Maslov, M. Roetteler, S. Debnath, C. Figgatt, K. A. Landsman, K. Wright, and C. Monroe, *Proceedings of the National Academy of Sciences* **114**, 3305 (2017).
- [23] C. Neill, P. Roushan, K. Kechedzhi, S. Boixo, S. V. Isakov, V. Smelyanskiy, R. Barends, B. Burkett, Y. Chen, Z. Chen, B. Chiaro, A. Dunsworth, A. Fowler, B. Foxen, R. Graff, E. Jeffrey, J. Kelly, E. Lucero, A. Megrant, J. Mutus, M. Neeley, C. Quintana, D. Sank, A. Vainsencher, J. Wenner, T. C. White, H. Neven, and J. M. Martinis, (2017), 1709.06678v1.
- [24] D. Wecker, M. B. Hastings, and M. Troyer, “Towards practical quantum variational algorithms,” (2015).
- [25] J. R. McClean, J. Romero, R. Babbush, and A. Aspuru-Guzik, *New Journal of Physics* **18**, 023023 (2016).
- [26] K. Temme, S. Bravyi, and J. M. Gambetta, (2017), 1612.02058v2.
- [27] Y. Li and S. C. Benjamin, *Physical Review X* **7** (2017), 10.1103/physrevx.7.021050.
- [28] A. Kandala, A. Mezzacapo, K. Temme, M. Takita, M. Brink, J. M. Chow, and J. M. Gambetta, *Nature* **549**, 242 (2017).
- [29] R. Babbush, N. Wiebe, J. McClean, J. McClain, H. Neven, and G. K.-L. Chan, (2017), 1706.00023v2.
- [30] L. Z. Stolarczyk and H. J. Monkhorst, *Mol. Phys.* **108**, 3067 (2010).
- [31] Z. Rolik and M. Kállay, *The Journal of Chemical Physics*

- 141**, 134112 (2014).
- [32] A. Signoracci, T. Duguet, G. Hagen, and G. R. Jansen, *Physical Review C* **91** (2015), <https://doi.org/10.1103/PhysRevC.91.064320>.
- [33] N. S. O. Attila Szabo, *Modern Quantum Chemistry* (Dover Publications Inc., 1996).
- [34] G. Rickayzen, *Green's Functions and Condensed Matter* (Academic Press, 1991).
- [35] D. Senechal, A.-M. Tremblay, and C. Bourbonnais, *Theoretical Methods for Strongly Correlated Electrons*, CRM Series in Mathematical Physics (Springer-Verlag New York, 2004).
- [36] A. J. Leggett, *Quantum Liquids* (Oxford University Press, 2006).
- [37] P. Ring and P. Schuck, *The nuclear many-body problem* (Springer-Verlag GmbH, 1980).
- [38] M. Bender, P.-H. Heenen, and P.-G. Reinhard, *Reviews of Modern Physics* **75**, 121 (2003).
- [39] B. Loiseau and Y. Nogami, *Nucl. Phys. B* **2**, 470 (1967).
- [40] C. V. Kraus, M. M. Wolf, J. I. Cirac, and G. Giedke, *Phys. Rev. A* **79** (2009), <https://doi.org/10.1103/PhysRevA.79.012306>.
- [41] C. V. Kraus and J. I. Cirac, *New J. Phys.* **12**, 113004 (2010).
- [42] L. N. Cooper, *Physical Review* **104**, 1189 (1956).
- [43] J. Bardeen, L. N. Cooper, and J. R. Schrieffer, *Physical Review* **106**, 162 (1957).
- [44] F. Verstraete, J. I. Cirac, and J. I. Latorre, *Phys. Rev. A* **79**, 032316 (2009).
- [45] C. Bloch and A. Messiah, *Nuclear Physics* **39**, 95 (1962).
- [46] L. G. Valiant, *SIAM Journal on Computing* **31**, 1229 (2002).
- [47] B. M. Terhal and D. P. DiVincenzo, *Phys. Rev. A* **65**, 032325 (2002).
- [48] S. B. Bravyi and A. Y. Kitaev, *Annals of Physics* **298**, 210 (2002).
- [49] R. Jozsa and A. Miyake, *Proc. R. Soc. A* **464**, 3089 (2008).
- [50] D. J. Brod, *Phys. Rev. A* **93**, 062332 (2016).
- [51] Z. Jiang, K. J. Sung, K. Kechedzhi, V. N. Smelyanskiy, and S. Boixo, arXiv preprint arXiv:1711.05395 (2017).
- [52] D. K. Hoffman, R. C. Raffanetti, and K. Ruedenberg, *Journal of Mathematical Physics* **13**, 528 (1972).
- [53] N. Khaneja, T. Reiss, C. Kehlet, T. Schulte-Herbrüggen, and S. J. Glaser, *Journal of Magnetic Resonance* **172**, 296 (2005).
- [54] S. Machnes, U. Sander, S. J. Glaser, P. de Fouquières, A. Gruslys, S. Schirmer, and T. Schulte-Herbrüggen, *Physical Review A* **84** (2011), [10.1103/PhysRevA.84.022305](https://doi.org/10.1103/PhysRevA.84.022305).
- [55] P. Jordan and E. Wigner, *Z. Phys.* **47**, 631 (1928).
- [56] J. T. Seeley, M. J. Richard, and P. J. Love, *J. Chem. Phys.* **137**, 224109 (2012).
- [57] M. B. Hastings, D. Wecker, B. Bauer, and M. Troyer, *Quantum Info. Comput.* **15** (2015).
- [58] J. Romero, R. Babbush, J. R. McClean, C. Hempel, P. Love, and A. Aspuru-Guzik, (2017), [1701.02691v1](https://arxiv.org/abs/1701.02691).
- [59] T. Shi, E. Demler, and J. I. Cirac, (2017), [1707.05902v1](https://arxiv.org/abs/1707.05902).
- [60] T. G. Kolda, R. M. Lewis, and V. Torczon, *SIAM Rev.* **45**, 385 (2006).
- [61] J. R. McClean, R. Babbush, P. J. Love, and A. Aspuru-Guzik, *Journal of Physical Chemistry Letters* **5**, 4368 (2014).
- [62] P.-L. Dallaire-Demers and F. K. Wilhelm, *Physical Review A* **94** (2016), [10.1103/physreva.94.062304](https://doi.org/10.1103/physreva.94.062304).
- [63] R. Pariser and R. G. Parr, *The Journal of Chemical Physics* **21**, 466 (1953).
- [64] R. Pariser and R. G. Parr, *The Journal of Chemical Physics* **21**, 767 (1953).
- [65] J. A. Pople, *Transactions of the Faraday Society* **49**, 1375 (1953).
- [66] J. Hubbard, *Proceedings of the Royal Society of London. Series A, Mathematical and Physical Sciences* **276**, 238 (1963).
- [67] E. H. Lieb and F. Y. Wu, *Physica A* **321**, 1 (2003).
- [68] F. Essler, H. Frahm, F. Gohmann, A. Klumper, and V. E. Korepin, *The One-Dimensional Hubbard Model* (Cambridge University Press, 2005).
- [69] P. W. Anderson, *Science* **235**, 1196 (1987).
- [70] A. J. Leggett, *Proc. Natl. Acad. Sci. USA* **96**, 8365 (1999).
- [71] P. W. Anderson, P. A. Lee, M. Randeria, T. M. Rice, N. Trivedi, and F. C. Zhang, *J Phys. Condens. Matter* **16**, R755 (2004).
- [72] P. G. Szalay, T. Müller, G. Gidofalvi, H. Lischka, and R. Shepard, *Chemical Reviews* **112**, 108 (2012).
- [73] B. R. Arnold and J. Michl, *Kinetics and Spectroscopy of Carbenes and Biradicals* (Springer Us, 2013).
- [74] B. R. Arnold, J. G. Radziszewski, A. Champion, S. S. Perry, and J. Michl, *Journal of the American Chemical Society* **113**, 692 (1991).
- [75] B. R. Arnold and J. Michl, *The Journal of Physical Chemistry* **97**, 13348 (1993).
- [76] D. W. Whitman and B. K. Carpenter, *Journal of the American Chemical Society* **104**, 6473 (1982).
- [77] N. Mataga and K. Nishimoto, *Z. phys. Chem* **13**, 140 (1957).
- [78] T. G. Schmalz, L. Serrano-Andrés, V. Sauri, M. Merchán, and J. M. Oliva, *The Journal of Chemical Physics* **135**, 194103 (2011).
- [79] T. G. Schmalz, *Croatica Chemica Acta* **86**, 419 (2013).
- [80] M. Potthoff, M. Aichhorn, and C. Dahnken, *Phys. Rev. Lett.* **91**, 206402 (2003).
- [81] M. Potthoff, *Condens. Mat. Phys.* **9**, 557 (2006).
- [82] D. Senechal, "An introduction to quantum cluster methods," (2008), arXiv:cond-mat.str-el/0806.2690v2 [cond-mat.str-el].
- [83] D. Senechal, in *High Performance Computing Systems and Applications* (2008).
- [84] F. Herrera, Y. Cao, S. Kais, and K. B. Whaley, *New Journal of Physics* **16**, 075001 (2014).
- [85] M. A. Nielsen and I. L. Chuang, *Quantum Computation and Quantum Information* (Cambridge University Press, 2001).
- [86] T. Byrnes and Y. Yamamoto, *Phys. Rev. A* **73** (2006), <https://doi.org/10.1103/PhysRevA.73.022328>.
- [87] E. Zohar and M. Burrello, *Phys. Rev. D* **91**, 054506 (2015).
- [88] M. Dalmonte and S. Montangero, *Contemporary Physics* **57**, 388 (2016).